Turkish Journal of Chemistry

Volume 36 | Number 5 Article 5

1-1-2012

Preparation of porphyrinated polyacrylonitrile fiber mat supported TiO_2 photocatalyst and its photocatalytic activities

LINJUN SHAO

JI CHEN

LUYAO HE

GUIYING XING

WEIXI LV

See next page for additional authors

Preparation of porphyrinated polyacrylonitrile fiber mat supported TiO_2 photocatalyst and its photocatalytic activities

Authors
LINJUN SHAO, JI CHEN, LUYAO HE, GUIYING XING, WEIXI LV, ZAINA CHEN, and CHENZE QI

Turk J Chem
36 (2012) , 700 – 708.

doi:10.3906/kim-1112-32

Preparation of porphyrinated polyacrylonitrile fiber mat supported TiO_2 photocatalyst and its photocatalytic activities

Linjun SHAO, Ji CHEN, Luyao HE, Guiying XING, Weixi LV, Zaina CHEN, Chenze QI*

Institute of Applied Chemistry, Shaoxing University, Shaoxing, Zhejiang Province 312000, PEOPLE'S REPUBLIC OF CHINA

e-mail: qichenze@usx.edu.cn

Received: 14.12.2011

Fe(III)meso-tetraphenylporphyrinated polyacrylonitrile fiber mat supported TiO_2 photocatalyst (PANC/TiO_2 mat) was prepared via copolymerization and electrospinning. SEM images showed that well-defined fibers with diameters around 1.47 $\pm$ 0.26 μm were fabricated from Fe(III)meso-tetraphenylporphyrin (FeTPP)-acrylonitrile copolymer (PANC) and TiO_2 mixture. The XRD characterizations demonstrated that the electrospinning process had no effect on the anatase structure of TiO_2. The photocatalytic activity of the PANC/TiO_2 mat was examined for the photodegradation of methyl red in aqueous solution under the irradiation of visible light. The results showed that this PANC/TiO_2 fiber mat was very efficient for the photodegradation of methyl red, with a degradation percentage over 94%. It is worth noting that the PANC/TiO_2 mat could be easily recovered and reused 3 times without any destruction of fiber morphologies.

Key Words: Electrospinning, porphyrins, photodegradation, photolysis

Introduction

The treatment and purification of waste water is one of today's major concerns of both industrial and scientific activities. Precipitation, coagulation, flocculation, and adsorption have been widely used to remove pollutants from waste water in many cases, but they merely transfer pollutants from aqueous phase to solid phase, causing secondary pollution.[1–3] By constant, decomposition of pollutant by photocatalysis is a much more promising method for the treatment of polluted water.[4–6] As TiO_2-based photocatalysis could directly photodegrade

*Corresponding author

organic pollutants (e.g., alkanes, alcohols, phenols, dyes, and pesticides) into CO_2, H_2O, and innocuous inorganic species, the TiO_2-based photocatalysis system is one of the most potential photocatalysis systems for practical applications. Unfortunately, TiO_2 could only be activated by ultraviolet radiation (the wavelength of which is less than 387 nm), which greatly limits its application in largescale industries. Dye-sensitization is an effective way to extend the light absorption band of TiO_2 from the ultraviolet light region into the visible light region.[7,8] Porphyrins and metalloporphyrins, which can efficiently harvest sunlight and have high molar adsorption coefficients in the visible region and high quantum yields of photo-excited triplet states, are recognized as one of the best photosensitizers.[9−13] Furthermore, some metalloporphyrins themselves are excellent photocatalysts and so they can cooperate with TiO_2 participating in the photodegradation of organic pollutants.[11−13]

Electrospinning is a simple but efficient method for producing non-woven mats with large surface area to volume ratio and excellent mechanical strength. These electrospun mats can be used in various areas such as filtration, composite material, tissue engineering, and supporting material.[14,15] A number of synthetic, bio-related polymers and composites have been successfully fabricated into sub-micro- or nanofibers for various applications.[16,17] Park et al. have prepared pure TiO_2 fibers by electrospinning, but the poor mechanical stability greatly limited their application in waste water treatment.[18] In order to solve this problem, TiO_2 was supported onto the poly(dimethyl siloxane) fiber using hybrid electrospinning and sol-gel methods. This hybrid fiber mat was very effective to photodegrade methylene blue.[19] Uyar et al. have prepared a series of polymer [poly(methyl methacrylate), polyacrylonitrile, polyethylene terephthalate, polycarbonated] fiber mats as the supporting materials of TiO_2 short nanofibers. It was found that all these nanofibrous composites had photocatalytic activities. These fiber structures could increase the dispersion of active catalyst species and facilitate the recovery of catalyst.[20]

Among the polymers, acrylonitrile-based homo- and copolymers were the most widely used polymers due to their excellent spinnability and chemical stability.[21−22] Therefore, FeTPP-acrylonitrile copolymer (PANC) was electrospun into fiber mat as the supporting material in this study. FeTPP in the copolymer could act as the photosensitizer of TiO_2. The larger size of the fiber mat can greatly facilitate the recovery of photocatalyst and the FeTPP in the copolymer can efficiently extend the absorption band and enhance the molar adsorption coefficient of TiO_2. The PANC fiber mat supported TiO_2 mat (PANC/TiO_2 mat) has been demonstrated as an efficient and recyclable heterogeneous photocatalyst for photodegradation of methyl red in this article.

Experimental

Materials

Methyl red was purchased from Shanghai Yu'an Sixteenth Production Brigade Plant. Hydrogen peroxide (H_2O_2) (30 vol.%) was supplied by Sinopharm Chemical Reagent Co., Ltd. TiO_2 (anatase) particles were purchased from Shanghai Reagent Plant. Polyacrylonitrile (PAN) and FeTPP-acrylonitrile copolymer (FeTPP weight content: 1.25%) were synthesized and purified according to the literature method.[23]

Fabrication of PANC/TiO_2 hybrid fiber mat

PANC and TiO_2 were mixed with various polymers in certain weight ratio (95:5). The mixture was then dissolved in DMF at a concentration of 8 wt.%. Electrospinning was carried out on self-made electrospinning equipment. The polymer solution in a syringe was delivered through a needle tip (0.8 mm inner diameter) 12.0 cm away from the collector, by a micro-infusion pump (WZ-502C, Zhejiang University Medical Instrument Co., Ltd, China) at a constant rate of 1.0 mL/min. The syringe needle was directly connected to a 15 kV high voltage supply (GDW-a, Tianjin Dongwen High-voltage Power Supply Plant, China) and the collector was a sheet of aluminum foil. The residual solvent of the prepared fiber mats was removed under a reduced pressure at room temperature, and the resulting mats were stored in a desiccator until application.

General procedure for photodegradation of methyl red

The photocatalyzed oxidative degradation of methyl red was performed in a photochemical reactor (XPA-7, Nanjing Xujiang Electromechanical Plant, China). For this, 10 mg of photocatalyst and 15 mL of methyl red solution in deionized water (20 mg/L) were added to a tubular reactor and stirred for about 1 h prior to irradiation with a 40 W incandescent bulb at 40 °C, and then 1.0 mL H_2O_2 (0.65 mmol/L) was added to the solution just before the degradation reaction. After the reaction, the solution was transferred into a quartz cell for UV-Vis measurement.

Residue of methyl red in solution was calculated according to the following equation:

$$\text{Residue of methyl red } = [(A - A_t)/A] \times 100\%, \tag{1}$$

where A_t is the absorbance of methyl red (429 nm) at reaction time$t$, and A is the related initial absorbance.

Recycling and reuse of PANC/TiO_2 mat

The PANC/TiO_2 photocatalyst was removed from the reaction mixture by filtration, and the recycled photocatalyst was washed with distilled water and then reused for the next photodegradation reaction directly.

Characterization

The intrinsic viscosities $[\eta]$ of PAN and PANC were determined in DMF solution with a concentration of 1.0 mg/mL at 30 ± 0.5 °C using an Ubbelohde viscometer. UV-Vis spectra were recorded on a UV-1800 PC spectrometer (Mapada, China). The matched quartz cell path length was 1.0 cm. Morphologies of the electrospun mats were characterized using a scanning electron microscope (SEM) (Jeol, Jsm-6360lv, Japan). Samples for SEM analysis were sputtered with a 20-30 Å layer of Au to make them conductive. The diameter of the fibers was determined from the related SEM images and at least 50 fibers were counted. The X-ray diffraction (XRD) was recorded on an X-ray diffractometer (PANalytical, Empyrean, Netherlands).

Results and discussion

About 100 years ago, Fenton reported that Fe^{2+} ion could contribute to the formation of ·OH radical from H_2O_2; this is known as the photo-Fenton process (Path I).[24,25] Recently, Chu et al. reported that Fe^{3+} ion

could generate $\cdot O_2H$ radical via oxidation of H_2O_2 under the irridiation of UV light, while Fe^{3+} ion was reduced to Fe^{2+} ion, which was called the photo-Fenton-like process (Path II) (Figure 1).[26] These $\cdot OH$ and $\cdot O_2H$ radicals produced are the predominantly active species to degrade organic pollutants. Thus, FeTPP was chosen as the photosensitizer of TiO_2 in this study. The molecular structure and UV-Vis spectrum of PANC are shown in Figure 2. The porphyrin in PANC has a strong absorption peak at 413 nm (Soret band) and 2 less intensive peaks at 568 and 610 nm, which is consistent with the literature that the Q band of porphyrin strongly depends on the symmetry of the molecular structure.[27]

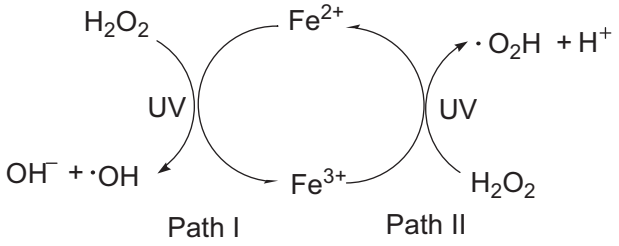

Figure 1. Photo-Fenton (Path I) and photo-Fenton-like (Path II) process.

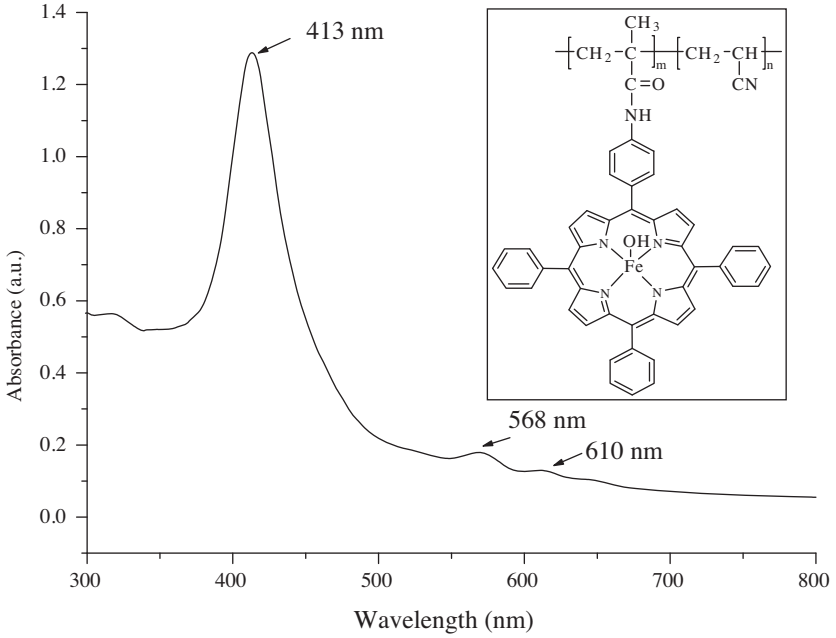

Figure 2. Molecular structure (inset) and UV-Vis spectrum of PANC.

It is well known that concentration plays an important role in electrospinning.[28] After examining a series of concentrations, 6 wt% of PAN in DMF was shown to be the best concentration to prepare uniform and homogeneous fibers. Therefore, 6 wt% polymer concentration was chosen for the subsequent fiber mats' preparation. As shown in Figure 3, all the fibers of mats were uniform and homogeneous. Because the intrinsic viscosity of PANC was 168 mL/g while that of PAN was only 144 mL/g, the fiber diameter of the PANC mat was larger than that of the PAN mat (Table 1). Since higher molecular weight could facilitate the preparation of uniform fibers and also increase the diameter of fibers, it is reasonable to get these results. Due to the insolubility

of TiO_2 in DMF, the fiber diameters of the PAN/TiO_2 mat and the PANC/TiO_2 mat were obviously increased compared to the fiber diameters of the corresponding PAN and PANC mats

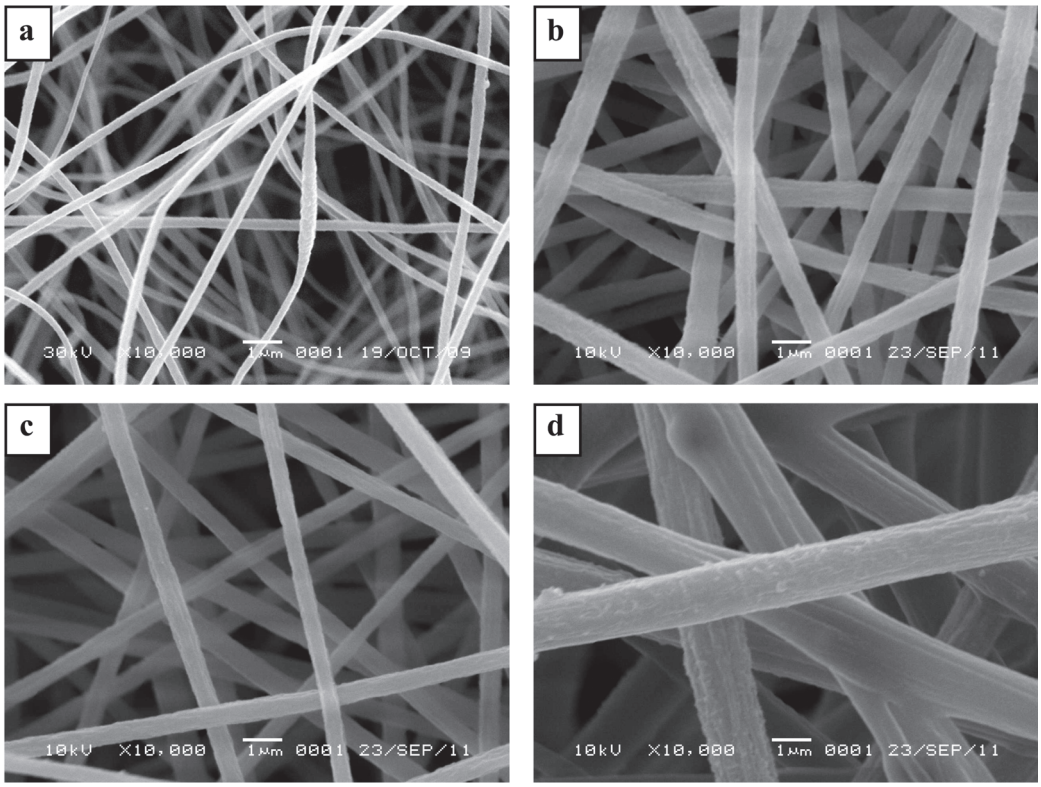

Figure 3. SEM images of PAN mat (a), PANC mat (b), PAN/TiO_2 mat (c), and PANC/TiO_2 mat (d).

Table 1. Fiber diameters of the electrospun mats.

Fiber mat	Diameter (nm)
PAN	231 ± 41
PAN/TiO_2	537 ± 86
PANC	572 ± 89
PANC/TiO_2	1470 ± 257

The crystalline structure of TiO_2 particles and PANC/TiO_2 mat was identified by X-ray diffraction (XRD). Figure 4 shows the XRD pattern of TiO_2 particles with series of diffraction peaks corresponding to anatase phase, which is known for its photocatalytic activity. As the content of TiO_2 in PANC/TiO_2 was only 5 wt.%, the corresponding XRD peak was very weak. However, the salient peak at $2\theta = 25^\circ$ corresponding to the (101) plane of anatase TiO_2 structure could be clearly identified. Therefore, the TiO_2 in PANC/TiO_2 was still in anatase structure and it can be concluded that the electrospinning process has no effect on the structure of TiO_2.

As methyl red has the framework of azo-dyes and azo-dyes are widely used in the textile and food industries, methyl red was employed to examine the photocatalytic activities of these electrospun mats (Figure

5). Due to the oxidation ability of H_2O_2, the methyl red was also degraded partly in the presence of the PAN mat. The photocatalytic activities of the PAN/TiO_2 fiber mat and PANC were comparative and higher than that of TiO_2 particles. However, the PANC/TiO_2 mat was obviously the most efficient photocatalyst, indicating the excellent photosensitization ability of FeTPP. In contrast to the literature,[29] the incorporation of TiO_2 into fibers could increase the photocatalytic activity of TiO_2. We think this might be due to 2 reasons: the first is that the incorporation of TiO_2 into the fiber could increase the dispersion of TiO_2 particles and avoid the aggregation of TiO_2 particles; the second is that the porous fiber mat could increase the adsorption capacity of dyes. As a result, the photocatalytic activities of the photocatalysts were reduced as follows: PANC/TiO_2 mat > PANC mat > PAN/TiO_2 mat> TiO_2 > PAN mat.

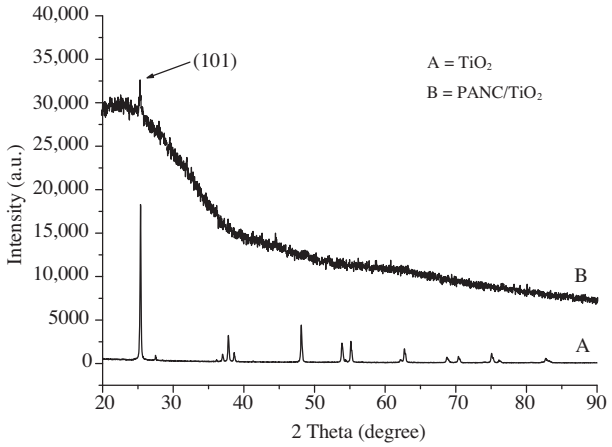

Figure 4. XRD patterns for TiO_2 (A) and PANC/TiO_2 mat (B).

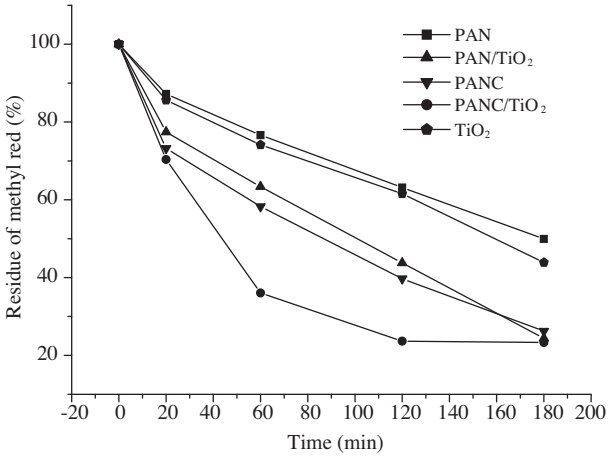

Figure 5. Photodegradation of methyl red as the function of irradiation time.

The amount of H_2O_2 was very important for photodegradation. It is reasonable to expect an increase in $\cdot$OH radical upon increment in H_2O_2. This in turn will increase the photodegradation rate and efficiency. As the concentration of H_2O_2 increased to 0.65 mol/L, further addition of H_2O_2 indeed could enhance the photodegradation efficiency after 3 h of irradiation (Figure 6). However, the photodegradation rate in the first hour of irradiation was reduced. A possible explanation could be that too much H_2O_2 would lead to the formation of peroxyl radical ($HO_2\cdot$), which is a much weaker oxidant than $\cdot$OH radical.[30] As a result, the degradation efficiency increased while the degradation rate decreased with the concentration of H_2O_2 being over 0.65 mol/L.

As the photocatalytic decomposition reaction is approximately first-order kinetic, the plot of $\ln C_0/C$ as a function of time gives a straight line.[31] Thus, the photocatalytic reaction can be simply described as Eq. (2):

$$\ln C_0/C = \ln A_0/A_t = kt, \tag{2}$$

where A_t is the absorbance of dyes (429 nm for methyl red) at time t, and A_0 is the initial absorbance prior to the reaction. C_0 is the original concentration of methyl orange and C is the concentration after irradiated for time t. k is the overall degradation rate constant, which demonstrated the photocatalytic activity of the photocatalyst under visible light. As shown in Table 2, the PANC/TiO_2 mat has the highest photocatalyst

activity. When the concentration of H_2O_2 is 0.97 mol/L, the degradation rate constant (k) of PANC/TiO_2 is 1.611×10^{-2} min^{-1} and the corresponding half-life time ($t_{1/2}$) is 43.03 min.

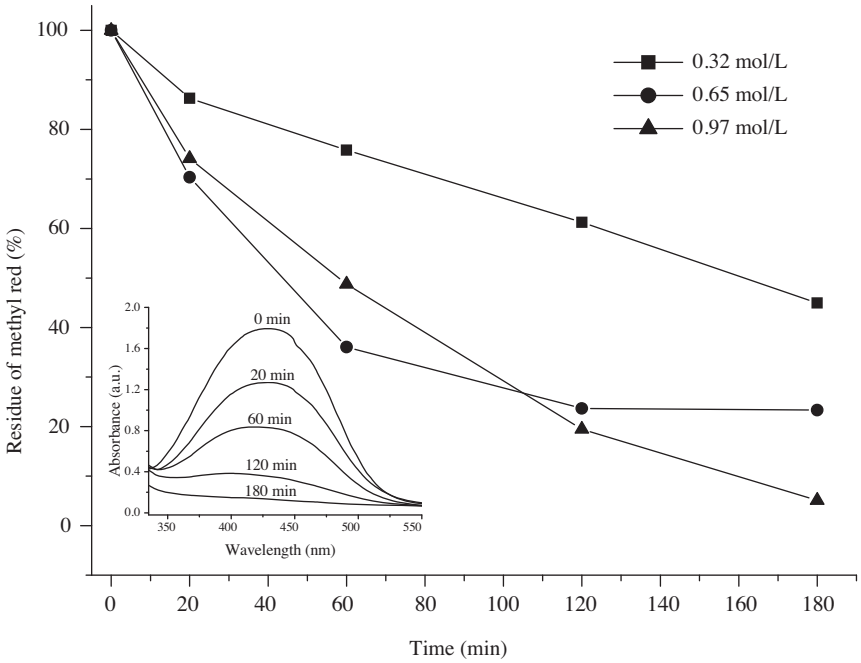

Figure 6. Effects of hydrogen peroxide concentration on methyl red photodegradation with PANC/TiO_2 mat as the photocatalyst. The inset shows the UV-Vis spectra of methyl red solutions as the function of irradiation time (H_2O_2: 0.97 mol/L).

Table 2. Photodegradation kinetic data of methyl orange.

Photocatalyst	H_2O_2 (mol/L)	R*	K (10^{-3} min)	$t_{1/2}$
TiO_2	0.65	0.992	4.27	155.69
PAN	0.65	0.996	3.67	188.87
PAN/TiO_2	0.65	0.992	8.16	84.94
PANC	0.65	0.993	7.36	94.18
PANC/TiO_2	0.65	0.922	7.01	98.88
PANC/TiO_2	0.32	0.995	4.20	165.04
PANC/TiO_2	0.97	0.991	16.11	43.03

* The R value of fitting curve.

Recovery and recycling of photocatalyst is a key factor relating to its cost and the prevention of secondary pollution of water. The prepared PANC/TiO_2 fiber mat photocatalyst is much easier to separate from the reaction mixture by filtration than powder catalyst because of the big size of the fiber mat. Unfortunately, the photocatalytic activity of PANC/TiO_2 decreased about 10% after each cycle, which might be due to the loss of

photocatalyst in the recovery step and the destruction of FeTPP ring in the photodegradation step (Table 3). However, the SEM images of the recovered PANC/TiO_2 mat showed that no changes in the fiber morphology occurred even after 3 cycles (Figure 7).

Table 3. Reuse of the PANC/TiO_2 mat.

Cycles	Photodegradation (%)
First	94.89
Second	86.94
Third	75.85

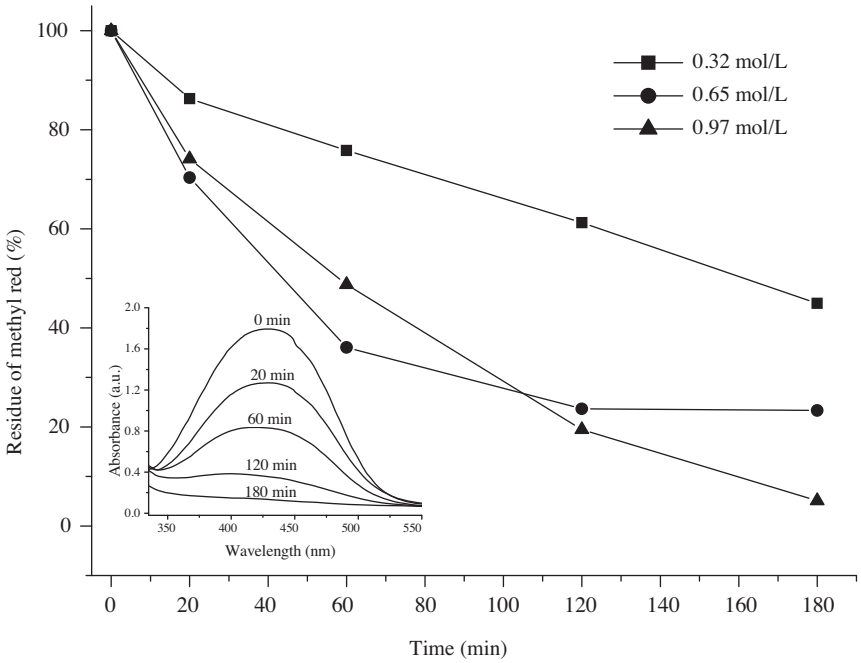

Figure 7. SEM images of the recovered PANC/TiO_2 mat recycled 3 times.

Acknowledgments

This work was supported by the Key Project of Shaoxing University (10LG1006), and the Zhejiang Science and Technology Innovation Team of Zhejiang Province Science and Technology Hall (2010 R 20014-16).

References

1. Soto, M. L.; Moure, A.; Parajo, J.C.; Dominguez, H. *J. Food Eng.* **2011**, *105*, 1-27.
2. Busca, G.; Berardinelli, S.; Resini, C.; Arrighi, L. *J. Hazard. Mater.* **2008**, *160*, 265-288.
3. Bhatnagar, A.; Vilar, V. J. P.; Botelho, C. M. S.; Boaventura, R. A. R. *Environ Technol.* **2011**, *32*, 231-249.

4. Sayılkan, F.; Asiltürk, M.; Şener, Ş.; Erdemoğlu, S.; Erdemoğlu, M.; Sayılkan, H. *Turk. J. Chem.* **2007**, *31*, 211-221.
5. Wang, C.; Li, J.; Mele, G.; Yang G. M.; Zhang, F. X.; Palmisano, L.; Vasapollo, G. *Appl. Catal. B: Environ.* **2007**, *76*, 218-226.
6. Pourahmad, A.; Sohrabnezhad, S.; Radaee, E. *J. Porous. Mat.* **2010**, *17*, 367-375.
7. Alex, S.; Santhosh, U.; Das, S. *J. Photoch. Photobio. A* **2005**, *172*, 63-71.
8. Gupta, S.; Tripathi, M. *Chinese. Sci. Bull.* **2011**, *56*, 1639-1657.
9. Wang, C.; Li, J.; Mele, G.; Duan, M. Y.; Lu, X. F.; Palmisano, L.; Vasapollo, G.; Zhang, F. X. *Dyes Pigments* **2010**, *84*, 183-189.
10. Granados-Oliveros, G.; Paez-Mozo, E. A.; Ortega, F. M.; Ferronato, C.; Chovelon, J. M. *Appl. Catal. B: Environ.* **2009**, *89*, 448-454.
11. Agarwala, A.; Bandyopadhyay, D. *Catal. Lett.* **2008**, *124*, 256-261.
12. Hequet, V.; Le Cloirec, P.; Gonzalez, C.; Meunier, B. *Chemosphere* **2000**, *41*, 379-386.
13. Kim, W.; Park, J.; Jo, H. J.; Kim H, -J.; Choi, W. *J. Phys. Chem. C* **2008,** *112*, 491-499.
14. Teo, W. E.; Ramakrishna, S. *Nanotechnolgoy* **2006**, *17*, 89-106.
15. Alves, A. K.; Berutti, F. A.; Bergmann, C. P. *J. Environ. Sci. Heal. A* **2009**, *44*, 835-840.
16. Huang, Z. M.; Zhang, Y. Z.; Kotaki, M.; Ramakrishna, S. *Compos. Sci. Technol.* **2003**, *63*, 2223-2253.
17. Beglou, M. J.; Haghi, A. K. *Cell. Chem. Technol.* **2008**, *42*, 441-462.
18. Son, W. K.; Cho, D.; Park, W. H. *Nanotechnology* **2006**, *17*, 439-443.
19. Kim, Y. B.; Cho, D. W.; Park, W. H. *J. Appl. Polym. Sci.* **2010**, *116*, 449-454.
20. Deniz, A. E.; Celebioglu, A.; Kayaci, F.; Uyar, T. *Mater. Chem. Phys.* **2011**, *129*, 701-704.
21. Dadvar, S.; Tavanai, H.; Dadvar, H.; Morshed, M.; Ghodsi, F. E. *J. Sol-Gel. Sci. Techn.* **2011**, *59*, 269-275.
22. Shao, L. J.; Liu, J.; Ye, Y. H.; Zhang, X. M.; Qi, C. Z. *Appl. Organometal. Chem.* **2011**, *25*, 699-703.
23. Wan, L. S.; Wu, J.; Xu, Z. K. *Macromol. Rapid Commun.* **2006,** *27*, 1533-1538.
24. Fenton, H. J. H. *J. Chem. Soc.* **1894**, *65*, 899-905.
25. Kim, Y. H.; Jung, Y. S.; Lim, W.T.; Park, J. Y. *Environ. Technol.* **2009**, *30*, 183-190.
26. Chu, W.; Kwan, C. Y.; Chan, K. H.; Kam, S. K. *J. Hazard. Mater.* **2005,** *121*, 119-126.
27. Gouterman, M. *The Porpyrins* (Vol III) [M], Academic Press, New York, 1978.
28. McKee, M. G.; Wilkes, G. L.; Colby, R. H.; Long, T. E. *Macromolecules* **2004**, *37*, 1760-1767.
29. Masocolo, G.; Comparelli, R.; Curri, M. L.; Lovecchio, G.; Lopez, A.; Agostiano, A. *J. Hazard. Mater.* **2007**, *142*, 130-137.
30. Chan, K. H.; Chu, W. *Appl. Catal. B: Environ.* **2005**, *58*, 157-163.
31. Li, X. Q.; Cheng, Y.; Kang, S. Z.; Mu, J. *Appl. Surf. Sci.* **2010**, *256*, 6705-6709.